HERON contains contributions based mainly on research work performed in I.B.B.C. and STEVIN and related to strength of materials and structures and materials science.

Jointly edited by:
STEVIN-LABORATORY
of the Department of
Civil Engineering of the
Delft University of Technology,
Delft, The Netherlands
and
I.B.B.C. INSTITUTE TNO
for Building Materials
and Building Structures,
Rijswijk (ZH), The Netherlands.

HERON vol. 26
1981
no. 2

Contents

GEOMETRICAL NON-LINEARITY IN COLLAPSE ANALYSIS OF THICK SHELLS, WITH APPLICATION TO TUBULAR STEEL JOINTS

R. S. Puthli

Institute TNO
for Building Materials and Building Structures
Lange Kleiweg 5, P.O. Box 49
2600 AA Delft, The Netherlands

GEOMETRICAL NON-LINEARITY IN COLLAPSE ANALYSIS OF THICK SHELLS, WITH APPLICATION TO TUBULAR STEEL JOINTS

Summary

Geometrical non-linearity is important, not only in problems involving elastic instability of thin structures, but also where they influence collapse in the material non-linear range involving thicker members. Using a continuum approach, this paper presents the basic principles of the general finite element formulation for thick shells that have been incorporated in an existing general purpose computer program suite DIANA with a very modular architecture [1]. The common assumptions of classical plate or shell theories have not been applied. Material non-linearity has only been mentioned briefly, where it involves plasticity in structural steel.

A comparison with the collapse analysis of a steel shell using conventional classical plate/shell theory is presented to illustrate variations that are ignored in classical theory. Experimental results on the collapse behaviour of a tubular steel T-joint are briefly compared with a numerical simulation, where the theoretical effects of geometric or material non-linearity alone are also presented.

Geometrical non-linearity in collapse analysis of thick shells, with application to tubular steel joints

1 Introduction

The analysis of plates and shells have in the past been carried out by formulations based upon classical thin plate Kirchhoff [2] theory, where shear deformation is ignored. This implies that normals to the mid-surface remains normal after deformation. This assumption is not suitable when moderately thick plate structures are also to be analysed, where shear deformation is not negligible. Mindlin [3] plate theory, sometimes referred to as Reissner [4] plate theory, allows for shear deformation, where normals remain straight, but not necessarily normal to the mid surface after deformation. The latter theory has been developed by Ahmad, Irons and Zienkiewicz [5] using assumed displacement based finite elements.

Ahmad et al. [5] use a degenerated three dimensional solid element and a "super-parametric" formulation, where the finite element formulated with simple coordinates in a parent element is "mapped" into a distorted form to a new curvilinear set when plotted in cartesian space. Curvatures in the plate and the element sides can thus be modelled. This approach has been modified for geometrical non-linearity and incorporated into the general purpose displacement based finite element computer program "DIANA", developed at the Institute for Building Materials and Building Structures (IBBC) of the Netherlands Centre of Applied Research (TNO). Although such modifications to include non-linearity to the degenerated shell formulations have recently been presented by Ramm [6], Krakeland [7] and Bathe et al. [8], it will be presented again in simplified matrix notation because of the ease of implementation in a computer program. Also, the presentation is deliberately simplified for users of the formulation with a basic knowledge of energy methods, calculus (including Taylor's expansion), vector and matrix algebra to follow the assumptions and limitations thoroughly. Reference should also be made to the book by Zienkiewicz [9]. The element formulation, including non-linearity, has been introduced without recourse to any classical plate or shell theory and treated in generality as in the analysis of continuum problems, where no assumptions are made on the magnitude of deformations or rotations. Therefore, large displacements or large rotations in any arbitrary direction of the shell can be modelled.

This paper only discusses the background pertaining to geometric non-linearity, with only the necessary details on material non-linearity mentioned, where relevant. The computer program DIANA uses a number of non-linear stress strain relationships to cover a large range of material behaviour that has been presented elsewhere [10].

Various bench mark tests have been carried out to check the formulation and some of the interesting comparisons are described.

2 Basic assumptions

1. The normals to the mid-surface remain straight after deformation and do not extend. By constraining the normals to remain straight, the error in shear deformation is small.
2. The strain energy corresponding to the stresses perpendicular to the mid-surface is ignored. This improves numerical conditioning by omitting the stiffness coefficients which become large when the shell thickness becomes small in comparison to the other dimensions of the element.

3 Coordinate transformations

Consider the typical thick shell element (Fig. 1) which is curved in and out of plane. Nodes "i" and thickness vector $\vec{V}_{3i}$ connecting the upper and lower points i_{top} and i_{bottom} across the thickness of the element at the boundaries prescribe the element shape. ξ and η are two curvilinear coordinates in the mid-span of the shell and ζ a linear coordinate in the thickness direction, which vary between -1 and 1 on their respective faces.

The relationship between the cartesian coordinates and the curvilinear coordinates are given by:

$$\begin{Bmatrix} x \\ y \\ z \end{Bmatrix} = \sum_{i=1}^{8} N_i \frac{(1+\zeta)}{2} \begin{Bmatrix} x_i \\ y_i \\ z_i \end{Bmatrix}_{\text{top}} + \sum_{i=1}^{8} N_i \frac{(1-\zeta)}{2} \begin{Bmatrix} x_i \\ y_i \\ z_i \end{Bmatrix}_{\text{bottom}} \tag{3.1}$$

where subscript "i" refers to a node number, and N_i is a function which is unity at node i and zero elsewhere.

N_i are derived as shape functions of a square parent element that satisfy compatibility at interfaces. Because the functions for the element with one mid-side node are parabolic in ξ and η, the sides of the element can take a parabolic form in x, y, z cartesian coordinates.

Expression (3.1) can be rewritten with respect to the mid-surface coordinates and a vector connecting the top and bottom surface nodes.

$$\begin{Bmatrix} x \\ y \\ z \end{Bmatrix} = \sum_{i=1}^{8} N_i \begin{Bmatrix} x_i \\ y_i \\ z_i \end{Bmatrix} + \sum_{i=1}^{8} N_i \frac{\zeta}{2} \vec{V}_{3i} \tag{3.2}$$

$$\begin{aligned} N_i &= \tfrac{1}{4}(1+\xi_0)(1+\eta_0)(\xi_0+\eta_0-1) \text{ for the corner nodes,} \\ &= \tfrac{1}{2}(1+\xi_0)(1-\eta^2) \text{ for mid-side nodes with } \xi_i = \pm 1,\ \eta_i = 0, \\ &= \tfrac{1}{2}(1-\xi^2)(1+\eta_0) \text{ for mid-side nodes with } \xi_i = 0,\ \eta_i = \pm 1 \end{aligned} \tag{3.3}$$

with $\xi_0 = \xi \cdot \xi_i$ and $\eta_0 = \eta \cdot \eta_i$

$$\vec{V}_{3i} = \begin{Bmatrix} x_i \\ y_i \\ z_i \end{Bmatrix}_{\text{top}} - \begin{Bmatrix} x_i \\ y_i \\ z_i \end{Bmatrix}_{\text{bottom}}$$

The above functions are quadratic in ξ and n as prescribed by the use of one mid-side node. Once this relationship between the cartesian and curvilinear coordinates is established, it would be easier to work with the curvilinear coordinates as the basis.

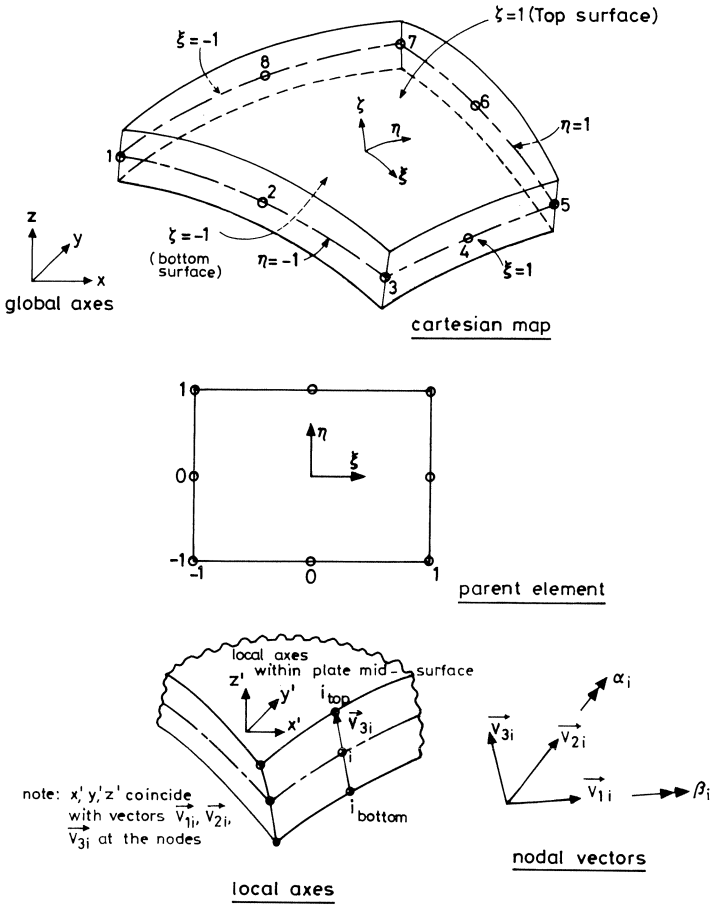

Fig. 1. Thick shell element.

4 Displacement field

In a three dimensional solid element, the element displacement functions would be defined by three cartesian (global) components of the displacement at each node of the element.

However, with the degenerated element, the displacement function is defined instead by the three cartesian (global) components of displacement u_i, v_i and w_i at the mid-surface nodes "i" and two orthogonal rotations of the thickness (or normal) vector $\vec{V}_{3i}$ (defined in section 3) about directions normal to it. In a plane perpendicular to $\vec{V}_{3i}$,

there are of course an infinite number of mutually perpendicular vectors. One of these directions $\vec{V}_{1i}$ is therefore arbitrarily chosen to be perpendicular to $\vec{V}_{3i}$ and the global x-axis. $\vec{V}_{2i}$ is therefore the other direction which is perpendicular to $\vec{V}_{3i}$ and $\vec{V}_{1i}$. If $\vec{V}_{3i}$ and the x-axis should coincide, the computer program checks for this parallellism and makes $\vec{V}_{1i}$ perpendicular to $\vec{V}_{3i}$ and the y-axis instead. As given in Fig. 1, the rotations of the normal vector $\vec{V}_{3i}$ about vectors $\vec{V}_{1i}$ and $\vec{V}_{2i}$ are defined as β_i and α_i in a clockwise direction.

The displacement field is therefore given as:

$$\begin{Bmatrix} u \\ v \\ w \end{Bmatrix} = \sum_{i=1}^{8} \left\{ N_i \begin{Bmatrix} u_i \\ v_i \\ w_i \end{Bmatrix} + N_i \frac{\xi}{2} [\vec{V}_{1i} - \vec{V}_{2i}] \begin{Bmatrix} \alpha_i \\ \beta_i \end{Bmatrix} \right\} \tag{4.1}$$

where u, v and w are cartesian (global) components of displacement within an element mid-surface and u_i, v_i, w_i, α_i and β_i are cartesian components of displacements and rotations of the shell element at mid-surface nodes i.

5 Definition of strains

A general definition of strains which is valid whether or not displacements or strains are large, require to be defined. For convenience in abridging notations, assume the cartesian coordinates in Fig. 2 to be given by x_1, x_2 and x_3, which in abridged form is x_i. Let coordinates of point A be x_1, x_2 and x_3 and a point B, infinitesimally close to A, $x_1 + \Delta x_1$, $x_2 + \Delta x_2$ and $x_3 + \Delta x_3$ in the initial configuration and X_1, X_2 and X_3 in the deformed configuration. With deformation of the body, A is displaced through u_1, u_2 and u_3, whereas B is displaced through $u_1 + \Delta u_1$, $u_2 + \Delta u_2$ and $u_3 + \Delta u_3$ along the cartesian axes. Δl and $\Delta l'$ are vectors of initial and deformated line length AB.

$$\begin{aligned} (\Delta l)^2 &= \Delta x_1^2 + \Delta x_2^2 + \Delta x_3^2 = \Delta x_i^2 \text{ (abridged form)} \\ (\Delta l')^2 &= (\Delta x_i + \Delta u_i)^2 \end{aligned} \tag{5.1}$$

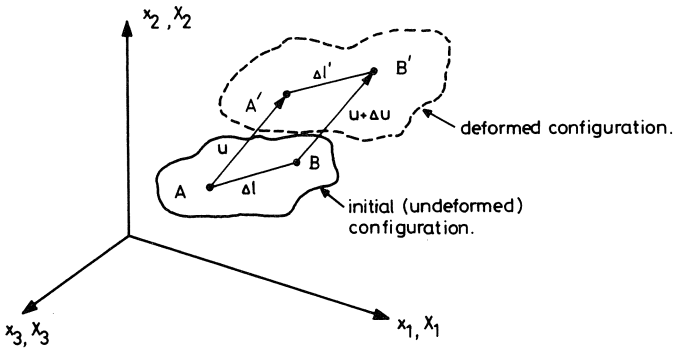

Fig. 2. Deformation of a body under load.

where all subscripts i (or j or k) infer 3 repeated operations with i or j or $k = 1, 2, 3$.

A measure of deformation is then:

$$(\Delta l')^2 - (\Delta l)^2 = 2\,\Delta x_i\;\Delta u_i + \Delta u_i\;\Delta u_i \tag{5.2}$$

Now, the Taylors series expansion of $u_i + \Delta u_i$ with the origin at u_i, is given by:

$$u_i + \Delta u_i = u_i + \Delta x_j \frac{\partial u_i}{\partial x_j} + \ldots \frac{(\Delta x_j)^n}{n!} \frac{\partial^n_{u_i}}{\partial^n_{x_j}} \tag{5.3}$$

Since the Δx_j are small, the non-linear parts of 5.3 may be truncated to give:

$$\Delta u_i = \frac{\partial u_i}{\partial x_j} \Delta x_j \tag{5.4}$$

Substituting (5.4) into (5.2) gives:

$$(\Delta l')^2 - (\Delta l)^2 = \frac{2\partial u_i}{\partial x_j}\;\Delta x_i\;\Delta x_j + \frac{\partial u_j}{\partial x_j}\frac{\partial u_i}{\partial x_k}\Delta x_j\;\Delta x_k \tag{5.5}$$

where k is introduced as a dummy subscript.

Replacing i by k on the right hand side of equation (5.5) as a dummy subscript and noting that:

$$\frac{\partial u_k}{\partial x_j}\Delta x_k\,\Delta x_j = \tfrac{1}{2}\left(\frac{\partial u_k}{\partial x_j} + \frac{\partial u_j}{\partial x_k}\right)\Delta x_j\,\Delta x_k \tag{5.6}$$

we get

$$(\Delta l')^2 - (\Delta l)^2 = 2\varepsilon_{jk}\,\Delta x_j\,\Delta x_k \tag{5.7}$$

where

$$\varepsilon_{jk} = \tfrac{1}{2}\left(\frac{\partial u_k}{\partial x_j} + \frac{\partial u_j}{\partial x_k}\right) + \tfrac{1}{2}\frac{\partial u_i}{\partial x_j}\frac{\partial u_i}{\partial x_k} = \varepsilon_{kj} \tag{5.8}$$

In unabridged notation, two of the nine equations (5.8) are:

$$\varepsilon_{xx} = \frac{\partial u}{\partial x} + \tfrac{1}{2}\left[\left(\frac{\partial u}{\partial x}\right)^2 + \left(\frac{\partial v}{\partial x}\right)^2 + \left(\frac{\partial w}{\partial x}\right)^2\right] \tag{5.8a}$$

$$\varepsilon_{xy} = \tfrac{1}{2}\left(\frac{\partial u}{\partial y} + \frac{\partial v}{\partial x}\right) + \tfrac{1}{2}\left[\frac{\partial u}{\partial x}\frac{\partial u}{\partial y} + \frac{\partial v}{\partial z}\frac{\partial v}{\partial y} + \frac{\partial w}{\partial x}\frac{\partial w}{\partial y}\right] = \tfrac{1}{2}\gamma_{xy} \tag{5.8b}$$

where u, v, w are the x, y, z components of displacement and γ_{xy} etc. are called the engineering shear strains. Now, defining a unit elongation of the initial infinitesimal length Δl by e, we get

$$e = \frac{\Delta l' - \Delta l}{\Delta l} \tag{5.9}$$

$$\text{now } e + \tfrac{1}{2}e^2 = \tfrac{1}{2}[(\Delta l')^2 - (\Delta l)^2]/\Delta l^2 \tag{5.10}$$

Substituting from 5.7 into 5.10:

$$e+\tfrac{1}{2}e^2=\varepsilon_{jk}\,\Delta x_j\,\Delta x_k/\Delta l^2 \tag{5.11}$$

Now

$$\frac{\Delta x_j}{\Delta l}=\lambda_j,\qquad \frac{\Delta x_u}{\Delta l}=\lambda_k,$$

where λ_j and λ_k are direction cosines of Δl relative to the x_j and x_k axes. Therefore,

$$e+\tfrac{1}{2}e^2=\varepsilon_{jk}\lambda_j\lambda_k \tag{5.12}$$

Unit elongation e is a definite quantity that is independent of the coordinate orientation for a given deformation. Therefore $\varepsilon_{jk}\lambda_j\lambda_k$ is invariant with respect to rotation of axes.

ε_{jk} are therefore components of a second order tensor, formulated by Green and St. Venant and is called Green's strain tensor. They are expressed as functions of the coordinates of the initial undeformated state, i.e., the so called Lagrangian coordinates.

Similarly, expressions for strain may be formed as functions of the coordinates of the deformed state, the so-called Eulerian coordinates. This form is attributed to Cauchy for infinitesimal strain and to Almansi and Hamel for finite strain. It is often called Almansi strain and is given as:

$$\eta_{jk}=\tfrac{1}{2}\left[\frac{\partial u_k}{\partial X_j}+\frac{\partial u_j}{\partial X_k}+\frac{\partial u_i}{\partial X_j}\,\frac{\partial u_i}{\partial X_k}\right]=\eta_{kj} \tag{5.13}$$

where X_i are the deformed coordinates.

If the components of displacement u_i are such that their first derivatives are small compared to unity,

$$\text{i.e. } \frac{\partial u_k}{\partial x_j}\ll 1\qquad \frac{\partial u_k}{\partial X_j}\ll 1 \tag{5.14}$$

then the squares and products of the partial derivatives of u_i are negligible, and n_{ij} reduces to Cauchy's infinitesimal strain tensor,

$$n_{jk}=\tfrac{1}{2}\left[\frac{\partial u_k}{\partial x_j}+\frac{\partial u_j}{\partial u_k}\right] \tag{5.15}$$

so that in the case of infinitesimal displacement, the distinction between Eulerian and Lagrangian coordinates disappears when expressing strain.

Since this paper deals with the numerical formulation where an initial (or total) Lagrangian coordinate system is used, the Eulerian system has only been mentioned briefly.

6 Green-Lagrange strains in element

Because of the basic assumptions, the strains have to be related in directions of orthogonal axes to the surface $\zeta=$ constant. Thus z' represents a normal to the surface

and x', y' two other orthogonal axes tangent to it (Fig. 1). Therefore, x', y', z' are considered to be parallel to vectors $\vec{V}_1$, $\vec{V}$, $\vec{V}_3$ respectively; u', v', w' represent displacements along the local axes x', y', z' respectively. $\vec{V}_1$, $\vec{V}_2$, $\vec{V}_3$ respresent vectors within an element mid-surface whereas $\vec{V}_{1i}$, $\vec{V}_{2i}$, $\vec{V}_{3i}$ represents values at mid-surface nodes i.

The strains are given by:

$$\{\varepsilon'\} = \{\varepsilon'_L\} + \{\varepsilon'_{NL}\} \tag{6.1}$$

where:

$$\{\varepsilon'\} = \begin{Bmatrix} \varepsilon_{x'} \\ \varepsilon_{y'} \\ \varepsilon_{z'} \\ \gamma_{x'y'} \\ \gamma_{y'z'} \\ \gamma_{z'x'} \end{Bmatrix} \tag{6.2}$$

$$\{\varepsilon'_L\} = \begin{Bmatrix} \partial u'/\partial x' \\ \partial v'/\partial y' \\ \partial w'/\partial z' \\ \partial u'/\partial y' + \partial v'/\partial x' \\ \partial v'/\partial z' + \partial w'/\partial y' \\ \partial w'/\partial x' + \partial u'/\partial z' \end{Bmatrix} \tag{6.3}$$

and:

$$\{\varepsilon'_{NL}\} = \begin{Bmatrix} \frac{1}{2}(\partial u'/\partial x')^2 + \frac{1}{2}(\partial v'/\partial x')^2 + \frac{1}{2}(\partial w'/\partial x')^2 \\ \frac{1}{2}(\partial u'/\partial y')^2 + \frac{1}{2}(\partial v'/\partial y')^2 + \frac{1}{2}(\partial w'/\partial y')^2 \\ \frac{1}{2}(\partial u'/\partial z')^2 + \frac{1}{2}(\partial v'/\partial z')^2 + \frac{1}{2}(\partial w'/\partial z')^2 \\ (\partial u'/\partial x')(\partial u'/\partial y') + (\partial v'/\partial x')(\partial v'/\partial y') + (\partial w'/\partial x')(\partial w'/\partial y') \\ (\partial u'/\partial y')(\partial u'/\partial z') + (\partial v'/\partial y')(\partial v'/\partial z') + (\partial w'/\partial y')(\partial w'/\partial z') \\ (\partial u'/\partial x')(\partial u'/\partial z') + (\partial v'/\partial x')(\partial v'/\partial z') + (\partial w'/\partial x')(\partial w'/\partial z') \end{Bmatrix} \tag{6.4}$$

$\partial u'/\partial x'$, etc. represent strains in the local axes x', y', z'. The strain in direction z', although present to facilitate transformations between the various coordinate systems, is neglected. Since none of these directions coincide with the global Cartesian coordinates x, y, z or the curvilinear coordinates ξ, n, ζ, a relationship must be established.

7 Determination of transformation matrices and vectors

The displacements (4.1) are given with reference to the curvilinear coordinates. The derivatives of these displacements with respect to the global x, y, z coordinates are given by:

$$\begin{bmatrix} \partial u/\partial x & \partial v/\partial x & \partial w/\partial x \\ \partial u/\partial y & \partial v/\partial y & \partial w/\partial y \\ \partial u/\partial z & \partial v/\partial z & \partial w/\partial z \end{bmatrix} = [J]^{-1} \begin{bmatrix} \partial u/\partial \xi & \partial v/\partial \xi & \partial w/\partial \xi \\ \partial u/\partial \eta & \partial v/\partial \eta & \partial w/\partial \eta \\ \partial u/\partial \zeta & \partial v/\partial \zeta & \partial w/\partial \zeta \end{bmatrix} \tag{7.1}$$

where the Jacobian matrix $[J]$ is defined as:

$$[J] = \begin{bmatrix} \partial x/\partial \xi & \partial y/\partial \xi & \partial z/\partial \xi \\ \partial x/\partial \eta & \partial y/\partial \eta & \partial z/\partial \eta \\ \partial x/\partial \zeta & \partial y/\partial \zeta & \partial z/\partial \zeta \end{bmatrix} \tag{7.2}$$

and is calculated from relationship (3.2) as follows:

$$[J] = \sum_{i=1}^{8} \begin{Bmatrix} \dfrac{\partial N_i}{\partial \xi} & \dfrac{\zeta}{2}\dfrac{\partial N_i}{\partial \xi} \\ \dfrac{\partial N_i}{\partial \eta} & \dfrac{\zeta}{2}\dfrac{\partial N_i}{\partial \eta} \\ 0 & \dfrac{N_i}{2} \end{Bmatrix} \begin{Bmatrix} x_i & y_i & z_i \\ \{\vec{V}_{3i}\}^T \end{Bmatrix} \tag{7.3}$$

Derivates of displacements with respect to global axes having been determined by (7.1), the transformation has to be carried out into the local axes x', y', z'. In order to do this, the thickness (or normal) vector $\vec{V}_3$ anywhere within the element has to be determined. At the nodes, $\vec{V}_3$ relates to the nodal thickness vectors $\vec{V}_{3i}$. Anywhere on the shell surface defined by (3.2), the tangents in direction parallel to the curvilinear coordinates are defined by their partial derivatives with respect to ξ and η.

The two vectors are therefore

$$\begin{Bmatrix} \partial x/\partial \xi \\ \partial y/\partial \xi \\ \partial z/\partial \xi \end{Bmatrix} \quad \text{and} \quad \begin{Bmatrix} \partial x/\partial \eta \\ \partial y/\partial \eta \\ \partial z/\partial \eta \end{Bmatrix}$$

The vector perpendicular to the plane defined by the above two vectors gives $\vec{V}_3$ and is:

$$\vec{V}_3 = \begin{bmatrix} \dfrac{\partial y}{\partial \xi}\dfrac{\partial z}{\partial \eta} - \dfrac{\partial y}{\partial \eta}\dfrac{\partial z}{\partial \xi} \\ \dfrac{\partial x}{\partial \eta}\dfrac{\partial z}{\partial \xi} - \dfrac{\partial x}{\partial \xi}\dfrac{\partial z}{\partial \eta} \\ \dfrac{\partial x}{\partial \xi}\dfrac{\partial y}{\partial \eta} - \dfrac{\partial x}{\partial \eta}\dfrac{\partial y}{\partial \xi} \end{bmatrix} \tag{7.4}$$

The orthogonal vectors $\vec{V}_1$ and $\vec{V}_2$ are determined as described in section 4 for nodal values $\vec{V}_{1i}$ and $\vec{V}_{2i}$.

The direction cosines λ_1, λ_2, λ_3 of each vector are determined by dividing values in

each vector by its scalar length. The scalar length is the square root of the sum of the squares of each of the three values in a vector.

The transformation matrix is given by:

$$[T] = [\{\lambda_1\}\{\lambda_2\}\{\lambda_3\}] \tag{7.5}$$

The local derivatives of the local orthogonal displacements may be obtained by the following operation:

$$\begin{bmatrix} \partial u'/\partial x' & \partial v'/\partial x' & \partial w'/\partial x' \\ \partial u'/\partial y' & \partial v'/\partial y' & \partial w'/\partial y' \\ \partial u'/\partial z' & \partial v'/\partial z' & \partial w'/\partial z' \end{bmatrix} = [T]^T \begin{bmatrix} \partial u/\partial x & \partial v/\partial x & \partial w/\partial x \\ \partial u/\partial y & \partial v/\partial y & \partial w/\partial y \\ \partial u/\partial z & \partial v/\partial z & \partial w/\partial z \end{bmatrix} [T] \tag{7.6}$$

The transformation matrix $[T]$ contains the direction cosines of x', y', z' with reference to the global axes. $[T]^T$ is the transpose of $[T]$.

The infinitesimal volume is given in terms of curvilinear coordinates as:

$$\mathrm{d}x\ \mathrm{d}y\ \mathrm{d}z = |J|\ \mathrm{d}\xi\ \mathrm{d}\eta\ \mathrm{d}\zeta \tag{7.7}$$

where $|J|$ = determinant of $[J]$.

8 Incremental strains

Rewriting initial strain in the abridged notation of (5.8),

$$\varepsilon_{ik} = \tfrac{1}{2}\left(\frac{\partial u_k}{\partial x_j} + \frac{\partial u_j}{\partial x_k}\right) + \tfrac{1}{2}\left(\frac{\partial u_i}{\partial x_j}\frac{\partial u_i}{\partial x_k}\right) \tag{8.1}$$

The deformed strain (see Fig. 2) is given by:

$$\begin{aligned} \varepsilon_{jk} + \Delta\varepsilon_{jk} = {} & \tfrac{1}{2}\left(\frac{\partial u_k}{\partial x_j} + \frac{\partial \Delta u_k}{\partial x_j} + \frac{\partial u_j}{\partial x_k} + \frac{\partial \Delta u_j}{\partial x_k}\right) \\ & + \tfrac{1}{2}\left(\frac{\partial u_i}{\partial x_j} + \frac{\partial \Delta u_i}{\partial x_j}\right)\left(\frac{\partial u_i}{\partial x_k} + \frac{\partial \Delta u_i}{\partial x_k}\right) \end{aligned} \tag{8.2}$$

Subtracting (8.1) from (8.2), we get incremental strain:

$$\Delta\varepsilon_{jk} = \tfrac{1}{2}\left(\frac{\partial \Delta u_k}{\partial x_j} + \frac{\partial \Delta u_j}{\partial x_k}\right) + \tfrac{1}{2}\left(\frac{\partial \Delta u_i}{\partial x_j}\frac{\partial u_i}{\partial x_k} + \frac{\partial u_i}{\partial x_j}\frac{\partial \Delta u_i}{\partial x_k}\right) + \tfrac{1}{2}\left(\frac{\partial \Delta u_i}{\partial x_j}\frac{\partial \Delta u_i}{\partial x_k}\right) \tag{8.3}$$

Since strains from the global axes are easily transformed into the local axes, all the following work will be expressed in global axes, particularly because stiffness formulations are also carried out in global axes. If $\partial u/\partial x$, etc. represent total strains and $\partial \Delta u/\partial x$ etc. the incremental strains, the total strains (6.1) or (8.1) may be expressed in matrix notation, using Engineering strain, as:

$$\{\varepsilon\} = \{\varepsilon_L\} + \{\varepsilon_{NL}\} \tag{8.4}$$

or

$$\{\varepsilon\} = \{\varepsilon_L\} + \tfrac{1}{2}[A]\{\theta\} \tag{8.5}$$

where $[A]$ is the matrix of the *total* slopes. i.e.,

$$[A] = \begin{bmatrix} \frac{\partial u}{\partial x} & \frac{\partial v}{\partial x} & \frac{\partial w}{\partial x} & 0 & 0 & 0 & 0 & 0 & 0 \\ 0 & 0 & 0 & \frac{\partial u}{\partial y} & \frac{\partial v}{\partial y} & \frac{\partial w}{\partial y} & 0 & 0 & 0 \\ 0 & 0 & 0 & 0 & 0 & 0 & \frac{\partial u}{\partial z} & \frac{\partial v}{\partial z} & \frac{\partial w}{\partial z} \\ \frac{\partial u}{\partial y} & \frac{\partial v}{\partial y} & \frac{\partial w}{\partial y} & \frac{\partial u}{\partial x} & \frac{\partial v}{\partial x} & \frac{\partial w}{\partial x} & 0 & 0 & 0 \\ 0 & 0 & 0 & \frac{\partial u}{\partial z} & \frac{\partial v}{\partial z} & \frac{\partial w}{\partial z} & \frac{\partial u}{\partial y} & \frac{\partial v}{\partial y} & \frac{\partial w}{\partial y} \\ \frac{\partial u}{\partial z} & \frac{\partial v}{\partial z} & \frac{\partial w}{\partial z} & 0 & 0 & 0 & \frac{\partial u}{\partial x} & \frac{\partial v}{\partial x} & \frac{\partial w}{\partial x} \end{bmatrix} \tag{8.6}$$

and,

$$\{\theta\} = \begin{Bmatrix} \frac{\partial u}{\partial x} \\ \frac{\partial v}{\partial x} \\ \frac{\partial w}{\partial x} \\ \frac{\partial u}{\partial y} \\ \frac{\partial v}{\partial y} \\ \frac{\partial w}{\partial y} \\ \frac{\partial u}{\partial z} \\ \frac{\partial v}{\partial z} \\ \frac{\partial w}{\partial z} \end{Bmatrix} \tag{8.7}$$

Using engineering strain, incremental strain (8.3) may be expressed in matrix notation as:

$$\{\Delta\varepsilon\} = \{\Delta\varepsilon_L\} + [A]\{\Delta\theta\} + \tfrac{1}{2}[\Delta A]\{\Delta\theta\} \tag{8.8}$$

where:

$$\{\Delta\varepsilon_L\} = \begin{Bmatrix} \partial\Delta u/\partial x \\ \partial\Delta v/\partial y \\ \partial\Delta w/\partial x \\ \partial\Delta u/\partial y + \partial\Delta v/\partial x \\ \partial\Delta v/\partial z + \partial\Delta w/\partial y \\ \partial\Delta w/\partial x + \partial\Delta u/\partial z \end{Bmatrix} \tag{8.9}$$

$$\{\Delta\theta\} = \begin{Bmatrix} \partial\Delta u/\partial x \\ \partial\Delta v/\partial x \\ \partial\Delta w/\partial x \\ \partial\Delta u/\partial y \\ \partial\Delta v/\partial y \\ \partial\Delta w/\partial y \\ \partial\Delta u/\partial z \\ \partial\Delta v/\partial z \\ \partial\Delta w/\partial z \end{Bmatrix} \tag{8.10}$$

and

$$[\Delta A] = \begin{bmatrix} \frac{\partial\Delta u}{\partial x} & \frac{\partial\Delta v}{\partial x} & \frac{\partial\Delta w}{\partial x} & 0 & 0 & 0 & 0 & 0 & 0 \\ 0 & 0 & 0 & \frac{\partial\Delta u}{\partial y} & \frac{\partial\Delta v}{\partial y} & \frac{\partial\Delta w}{\partial y} & 0 & 0 & 0 \\ 0 & 0 & 0 & 0 & 0 & 0 & \frac{\partial\Delta u}{\partial z} & \frac{\partial\Delta v}{\partial z} & \frac{\partial\Delta w}{\partial z} \\ \frac{\partial\Delta u}{\partial y} & \frac{\partial\Delta v}{\partial y} & \frac{\partial\Delta w}{\partial y} & \frac{\partial\Delta u}{\partial x} & \frac{\partial\Delta v}{\partial x} & \frac{\partial\Delta w}{\partial x} & 0 & 0 & 0 \\ 0 & 0 & 0 & \frac{\partial\Delta u}{\partial z} & \frac{\partial\Delta v}{\partial z} & \frac{\partial\Delta w}{\partial z} & \frac{\partial\Delta u}{\partial y} & \frac{\partial\Delta v}{\partial y} & \frac{\partial\Delta w}{\partial y} \\ \frac{\partial\Delta u}{\partial z} & \frac{\partial\Delta v}{\partial z} & \frac{\partial\Delta w}{\partial z} & 0 & 0 & 0 & \frac{\partial\Delta u}{\partial x} & \frac{\partial\Delta v}{\partial x} & \frac{\partial\Delta w}{\partial x} \end{bmatrix} \tag{8.11}$$

Equation (8.9) may be expressed in terms of the displacements and rotations at each node i, $(u_i, v_i, w_i, \alpha_i, \beta_i)$ where every subscript i denotes a sub-vector containing the total number of nodes. Equation (4.1) may first be rewritten as follows:

$$\begin{Bmatrix} u \\ v \\ w \end{Bmatrix} = N_i \begin{Bmatrix} u_i \\ v_i \\ w_i \end{Bmatrix} + N_i \frac{\zeta}{2} t_i \begin{Bmatrix} \lambda_{1xi} & -\lambda_{2xi} \\ \lambda_{1yi} & -\lambda_{2yi} \\ \lambda_{1zi} & -\lambda_{2zi} \end{Bmatrix} \begin{Bmatrix} \alpha_i \\ \beta_i \end{Bmatrix} \tag{8.12}$$

where

λ_{1xi} = the direction cosine of vector $\vec{V}_{1i}$ with respect to the global x axis at the i-th node, etc.

t_i = thickness, normal to the mid-surface of the shell and from section 7,

$$\vec{V}_{1i} = t_i \begin{Bmatrix} \lambda_{1xi} \\ \lambda_{1yi} \\ \lambda_{1zi} \end{Bmatrix} \tag{8.13}$$

$$\{\Delta \varepsilon_L\} = [B] \begin{Bmatrix} \Delta u_i \\ \Delta v_i \\ \Delta w_i \\ \Delta \alpha_i \\ \Delta \beta_i \end{Bmatrix} \tag{8.14}$$

where the strain displacement relationship $[B]$ is:

$$[B] = \begin{bmatrix} \frac{\partial N_i}{\partial x} & 0 & 0 & t_i \frac{\zeta}{2} \lambda_{1xi} \frac{\partial N_i}{\partial x} & -t_i \frac{\zeta}{2} \lambda_{2xi} \frac{\partial N_i}{\partial x} \\ 0 & \frac{\partial N_i}{\partial y} & & t_i \frac{\zeta}{2} \lambda_{1yi} \frac{\partial N_i}{\partial y} & -t_i \frac{\zeta}{2} \lambda_{2yi} \frac{\partial N_i}{\partial y} \\ 0 & 0 & \frac{\partial N_i}{\partial z} & t_i \frac{\zeta}{2} \lambda_{1zi} \frac{\partial N_i}{\partial z} & -t_i \frac{\zeta}{2} \lambda_{2zi} \frac{\partial N_i}{\partial z} \\ \frac{\partial N_i}{\partial y} & \frac{\partial N_i}{\partial x} & 0 & \begin{bmatrix} t_i \frac{\zeta}{2} \lambda_{1xi} \frac{\partial N_i}{\partial y} \\ + \frac{1}{2} \lambda_{1yi} \frac{\partial N_i}{\partial x} \end{bmatrix} & \begin{bmatrix} -t_i \frac{\zeta}{2} \lambda_{2xi} \frac{\partial N_i}{\partial y} \\ -t_i \frac{1}{2} \lambda_{2yi} \frac{\partial N_i}{\partial x} \end{bmatrix} \\ 0 & \frac{\partial N_i}{\partial z} & \frac{\partial N_i}{\partial y} & \begin{bmatrix} t_i \frac{\zeta}{2} \lambda_{1zi} \frac{\partial N_i}{\partial y} \\ + \frac{1}{2} \lambda_{1yi} N_i \end{bmatrix} & \begin{bmatrix} -t_i \frac{\zeta}{2} \lambda_{2zi} \frac{\partial N_i}{\partial y} \\ -t_i \frac{1}{2} \lambda_{2yi} N_i \end{bmatrix} \\ \frac{\partial N_i}{\partial z} & 0 & \frac{\partial N_i}{\partial x} & \begin{bmatrix} t_i \frac{\zeta}{2} \lambda_{1zi} \frac{\partial N_i}{\partial x} \\ + \frac{1}{2} \lambda_{1xi} N_i \end{bmatrix} & \begin{bmatrix} -t_i \frac{\zeta}{2} \lambda_{2zi} \frac{\partial N_i}{\partial x} \\ -t_i \frac{1}{2} \lambda_{2xi} N_i \end{bmatrix} \end{bmatrix} \tag{8.15}$$

(8.10) may be expressed in terms of displacements and rotations u_i, v_i, w_i, α_i, β_i at the nodes i as follows:

$$\{\Delta\theta\} = [G] \begin{Bmatrix} \Delta u_i \\ \Delta v_i \\ \Delta w_i \\ \Delta \alpha_i \\ \Delta \beta_i \end{Bmatrix} \tag{8.16}$$

where slope displacement relationship $[G]$ is:

$$[G] = \begin{bmatrix} \frac{\partial N_i}{\partial x} & 0 & 0 & t_i \frac{\zeta}{2} \lambda_{1xi} \frac{\partial N_i}{\partial x} & -t_i \frac{\zeta}{2} \lambda_{2xi} \frac{\partial N_i}{\partial x} \\ 0 & \frac{\partial N_i}{\partial x} & 0 & t_i \frac{\zeta}{2} \lambda_{1yi} \frac{\partial N_i}{\partial x} & -t_i \frac{\zeta}{2} \lambda_{2yi} \frac{\partial N_i}{\partial x} \\ 0 & 0 & \frac{\partial N_i}{\partial x} & t_i \frac{\zeta}{2} \lambda_{1zi} \frac{\partial N_i}{\partial x} & -t_i \frac{\zeta}{2} \lambda_{2zi} \frac{\partial N_i}{\partial x} \\ \frac{\partial N_i}{\partial y} & 0 & 0 & t_i \frac{\zeta}{2} \lambda_{1xi} \frac{\partial N_i}{\partial y} & -t_i \frac{\zeta}{2} \lambda_{2xi} \frac{\partial N_i}{\partial y} \\ 0 & \frac{\partial N_i}{\partial y} & 0 & t_i \frac{\zeta}{2} \lambda_{1yi} \frac{\partial N_i}{\partial y} & -t_i \frac{\zeta}{2} \lambda_{2yi} \frac{\partial N_i}{\partial y} \\ 0 & 0 & \frac{\partial N_i}{\partial y} & t_i \frac{\zeta}{2} \lambda_{1zi} \frac{\partial N_i}{\partial y} & -t_i \frac{\zeta}{2} \lambda_{2zi} \frac{\partial N_i}{\partial y} \\ \frac{\partial N_i}{\partial z} & 0 & 0 & t_i \frac{\zeta}{2} \lambda_{1xi} \frac{\partial N_i}{\partial z} & -t_i \frac{\zeta}{2} \lambda_{2xi} \frac{\partial N_i}{\partial z} \\ 0 & \frac{\partial N_i}{\partial z} & 0 & t_i \frac{\zeta}{2} \lambda_{1yi} \frac{\partial N_i}{\partial z} & -t_i \frac{\zeta}{2} \lambda_{2yi} \frac{\partial N_i}{\partial z} \\ 0 & 0 & \frac{\partial N_i}{\partial z} & t_i \frac{\zeta}{2} \lambda_{1zi} \frac{\partial N_i}{\partial z} & -t_i \frac{\zeta}{2} \lambda_{2zi} \frac{\partial N_i}{\partial z} \end{bmatrix} \tag{8.17}$$

Therefore, the incremental strains are given by:

$$\{\Delta\varepsilon\} = [H] \begin{Bmatrix} \Delta u_i \\ \Delta v_i \\ \Delta w_i \\ \Delta \alpha_i \\ \Delta \beta_i \end{Bmatrix} + \tfrac{1}{2}[\Delta A][G] \begin{Bmatrix} \Delta u_i \\ \Delta v_i \\ \Delta w_i \\ \Delta \alpha_i \\ \Delta \beta_i \end{Bmatrix} \tag{8.18}$$

where

$$[H] = [B] + [A][G] \tag{8.19}$$

The matrices $[A]$ and $[\Delta A]$ cannot be represented conveniently in terms of nodal displacements as shown for matrices $[B]$ and $[G]$. Each coefficient in these matrices is in-

dividually worked out by differentiating (8.12) and using *total* nodal displacements for $[A]$ and *incremental* nodal displacements for $[\Delta A]$.

For instance, coefficient A_{11} in $[A]$ is given by:

$$A_{11} = \frac{\partial u}{\partial x} = \left\{\frac{\partial f}{\partial x}\right\}_{11}^{T} \begin{Bmatrix} u_i \\ v_i \\ w_i \\ \alpha_i \\ \beta_i \end{Bmatrix} \tag{8.20}$$

where

$$\left\{\frac{\partial f}{\partial x}\right\}_{11}^{T} = \left\{\frac{\partial N_i}{\partial x} \quad 0 \quad 0 \quad t_i \frac{\zeta}{2} \lambda_{1xi} \frac{\partial N_i}{\partial x} \quad - t_i \frac{\zeta}{2} \lambda_{2xi} \frac{\partial N_i}{\partial x}\right\} \tag{8.21}$$

Similarly, coefficient ΔA_{11} in $[\Delta A]$ is given by

$$\Delta A_{11} = \frac{\partial \Delta u}{\partial x} = \left\{\frac{\partial f}{\partial x}\right\}_{11}^{T} \begin{Bmatrix} \Delta u_i \\ \Delta v_i \\ \Delta w_i \\ \Delta \alpha_i \\ \Delta \beta_i \end{Bmatrix} \tag{8.22}$$

9 Numerical determination of non-linear strain

Since the non-linear load deflection path is obtained numerically by means of piecewise incremental linear steps, the manner of obtaining Green-Lagrange strains or Almansi strains (in Eulerian coordinates) require to be mentioned.

a. *The Initial or Total Lagrange (TL) formulation*
The strains are referenced to the original undeformed coordinates and therefore every increment of strain represents the true Green-Lagrange strains. This method is used in the current work since it offers advantages because of the initial configuration occupying a fixed and stationary base.

b. *The Updated Lagrange (UL) formulation*
A true Almansi strain using Eulerian coordinates requires the coordinates of the unknown future configuration. The numerical procedure therefore only provides for strains based upon the last known configuration (i.e. the last incremental values). This is therefore known as an updated Lagrange formulation, since the approach determines Green-Lagrangian incremental strains of the new (unknown) configuration, but with the last known incremental configuration as a base.

So long as the strain is small as in most shell problems, analyses with large deflections

(or rotations) exhibit negligible differences between the prediction of TL and UL formulations [8].

10 Incremental stresses

The stresses associated with Green-Lagrange strains are called Piola-Kirchhoff stresses. The constitutive equations in the Total Lagrangian formulations (see section 9) relate Green-Lagrange strains to Piola-Kirchhoff stresses. The updated Lagrangian formulation relates the Almansi strains to Cauchy stresses (see section 5) when the strains are small. The present discussion being limited to the TL formulation, the stresses are Piola-Kirchhoff stresses. Each incremental stress component is added to the sum of all previous incremental stresses.

The incremental strains in the local axes $\{\Delta\varepsilon'\}$ (see transformation relationship 7.6) are stored and used to calculate the incremental stresses from the constitutive stress-strain relationship.

$$\{\Delta\sigma'\} = [E^*(\sigma)]\{\Delta\varepsilon'\} \tag{10.1}$$

where $[E^*(\sigma)]$ is the tangential elasto-plastic modular matrix which is a function of the current stress level in the materially non-linear stages of the analysis. However, with isotropic materials such as steel in the elastic region (prior to yield) it is given by:

$$[E^*(\sigma)] = \frac{E}{(1-\nu^2)} \begin{bmatrix} 1 & \nu & 0 & 0 & 0 & 0 \\ & 1 & 0 & 0 & 0 & 0 \\ & & 0 & 0 & 0 & 0 \\ & & & \frac{1-\nu}{2} & 0 & 0 \\ & \text{sym.} & & & \frac{1-\nu}{2k} & 0 \\ & & & & & \frac{1-\nu}{2k} \end{bmatrix} \tag{10.2}$$

where E and ν are the modulus of elasticity and Poisson's ratio respectively. "k" is a factor for improving the shear displacement approximation which is implied to be constant through the thickness due to the displacement function. Since the correct shear distribution is parabolic, $k = 1.2$ gives a more accurate representation of the correct strain energy, implying that the effective transverse shear modulus is $G/1.2$, where

$$G = \frac{E}{2(1+\nu)}$$

This is because the strain energy is obtained from the mean squared stress, whereas the shear load is obtained from the mean stress. The shear stress at a given height above the neutral axis is

$$\tau = \frac{V}{I} A \; e \tag{10.3}$$

where

V = shear force per unit width at cross section considered
I = second moment of area per unit width about the neutral axis
A = area of cross section above the given height
e = distance of center of area A from neutral axis

Now, if

t = thickness of plate at cross-section considered
z = distance to the given height where shear stress is required,

$$t = 2(t/2 - e) + z \tag{10.4}$$

from which:

$$e = z/2 \tag{10.5}$$

and

$$A = 2(t/2 - e) = t - z \tag{10.6}$$

Therefore,

$$\tau = \frac{v}{t^3/12}(t-z)z/2 \quad \text{or} \quad \tau = \frac{6Vz(t-z)}{t^3} \tag{10.7}$$

The shear strain energy per unit face area is given by

$$\tfrac{1}{2}\int_0^t \frac{\tau^2\,dz}{G} = \frac{1}{2G}\int_0^t \frac{36V^2z^2(t-z)^2}{t^6}\,dz = \frac{1\cdot 2V^2}{2Gt} \tag{10.8}$$

The shear strain energy based upon a uniform shear through the thickness is $V^2/2Gt$. Hence the correction to the shear modulus, giving on effective value of $G/1.2$.

11 Material non-linearity

In the ultimate strength analysis of shells, the coupled effect of large displacements and material non-linear behaviour is of fundamental importance. The formulation used in the present investigation uses the Prandtl-Reuss flow rules and the Von Mises yield criterion.

The basic approach to the problem, including the more generalized application to material non-linearity as applied within computer program DIANA, is presented by Kusters [10], who also describes the detailed Newton-Raphson and modified Newton-Raphson iteration procedure. The procedure is similar to that presented by Nayak and Zienkiewicz [14]. Both references give the approach used in monitoring the stress on the yield surface.

12 Stiffness formulation

The variational principle of minimum potential energy is used in the formulation, where the potential energy is stationary with regard to all kinematically admissible variations in displacements from the state of equilibrium. The potential energy of the shell (ignoring body forces) is given by:

$$\Pi = U - V \tag{12.1}$$

where strain energy U is given by:

$$U = \int_{\text{vol}} \int \int \left(\int_{\varepsilon_0}^{\varepsilon_1} \sigma \, d\varepsilon \right) \text{dvol} \tag{12.2}$$

and work "V" due to applied loads "P" over a surface "S" by

$$V = \int_S P(\delta - \delta_0) \, dS \tag{12.3}$$

An increment of the total potential energy is given by:

$$\Delta\Pi = \int_{\text{vol}} \int \int [\{\sigma\}^T\{\Delta\varepsilon\} + \tfrac{1}{2}\{\Delta\sigma\}^T\{\Delta\varepsilon\}] \, \text{dvol}$$

$$- \int_S (P + \Delta P) \, \Delta\delta \, dS - \int_S P(\delta - \delta_0) \, dS \tag{12.4}$$

where the last term may be ignored, since variations with respect to $\Delta\delta$ makes the term zero.

Introducing the global stress-strain relationship by transforming (10.1) into global axes, we get:

$$\Delta\Pi = \int_{\text{vol}} \int \int \{\sigma\}^T\{\Delta\varepsilon\} \, \text{dvol} + \tfrac{1}{2} \int_{\text{vol}} \int \int \{\Delta\varepsilon\}^T[E^*(\sigma)]\{\Delta\varepsilon\} \, \text{dvol}$$

$$- \int_S [(U + \Delta U)\Delta u + (V + \Delta V)\Delta v + (W + \Delta W)\Delta w] \, \text{dvol} \tag{12.5}$$

where U, V, W are components of applied load P and u, v, w are components of displacements δ in the global x, y and z directions respectively.

Now for stable equilibrium, the stationary value of the potential energy is an absolute minimum, i.e.,

$$\delta(\Delta\Pi) = 0 \tag{12.6}$$

substituting (8.18) into (12.5) and applying the variation:

$$\begin{Bmatrix} U \\ V \\ W \end{Bmatrix} + \begin{Bmatrix} \Delta U \\ \Delta V \\ \Delta W \end{Bmatrix} - \{ \int_{\text{vol}} \int \int [H]^T\{\sigma\} \, \text{dvol} \} = [K]\{\Delta\delta\} \tag{12.7}$$

where:

$$[K] = \int_{\text{vol}} \int \int [H]^T[E^*(\sigma)][H] \, \text{dvol} + \int_{\text{vol}} \int \int [G]^T[\sigma^*][G] \tag{12.8}$$

and:

$$[\sigma^*] = \begin{bmatrix} \sigma_x & 0 & 0 & \sigma_{xy} & 0 & 0 & \sigma_{xz} & 0 & 0 \\ & \sigma_x & 0 & 0 & \sigma_{xy} & 0 & 0 & \sigma_{xz} & 0 \\ & & \sigma_x & 0 & 0 & \sigma_{xy} & 0 & 0 & \sigma_{xz} \\ & & & \sigma_y & 0 & 0 & \sigma_{yz} & 0 & 0 \\ & & & & \sigma_y & 0 & 0 & \sigma_{yz} & 0 \\ & \text{sym.} & & & & \sigma_y & 0 & 0 & \sigma_{yz} \\ & & & & & & \sigma_z & 0 & 0 \\ & & & & & & & \sigma_z & 0 \\ & & & & & & & & \sigma_z \end{bmatrix} \tag{12.9}$$

(12.7) can be written as:

$$\{P_e\} + \{\Delta P_e\} - \{P_i\} = [K]\{\Delta\delta\} \tag{12.10}$$

where $\{P_e\} - \{P_i\}$ gives the out of balance load vector between the externally applied load and the internal stresses calculated from the displacements. When this term vanishes after a number of iterations exact equilibrium has been achieved for the current load increment $\{\Delta P_e\}$.

13 Integration of the stiffness matrix

a. *Gauss Quadrature*

Once the stiffness matrix for each element has been formed in turn, it can be integrated segmentally, element by element. A number of Gauss (or sampling) points are chosen, whose positions are allocated to achieve best accuracy. These Gauss points are therefore positions where the function is defined with the best accuracy. If the number of Gauss points in any direction is "n", its function as well as its position are unknown, giving $2n$ unknown. Therefore, a polynomial up to a degree $2n-1$ could be exactly integrated.

The Gauss rules are expressed below for a single integration up to surds of $n=3$ which are the ones most commonly used.

$$\begin{aligned} F = \int_{-1}^{1} f(\xi)\, d\xi &= 2f(\xi=0) \quad \text{when} \quad n=1 \\ &= f(\xi=-1/\sqrt{3}) + f(\xi=1/\sqrt{3}) \quad \text{when} \quad n=2 \\ &= \tfrac{5}{9} f(\xi=-\sqrt{0.6}) + \tfrac{8}{9} f(\xi=0) + \tfrac{5}{9} f(\xi=\sqrt{0.6}) \quad \text{when} \quad n=3 \end{aligned}$$

With area or volume integrals, the inner integral is evaluated first, keeping all other variables constant and the outer integrals evaluated successively in a similar manner.

The stiffness matrix of each Gauss point is evaluated and all contributions summed to form the overall element matrix. Strains and stresses are evaluated at each of the 4 Gauss points ($n=2$) or 9 Gauss points ($n=3$) for each element in the $\xi - n$ surface of the plate (see Fig. 3 for positions on the present element). The choice of the surface integra-

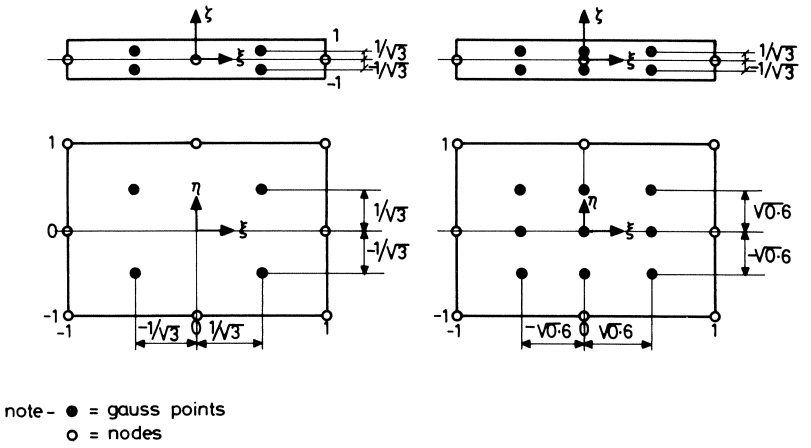

note - ● = gauss points
o = nodes

Fig. 3. Four and nine Gauss point integration station position in $\xi - \eta$ surface of parent element.

tion (4 or 9 Gauss points) is left to the user. The variation of the strain quantities in the ζ direction are linear, and therefore only two Gauss points are required in that direction for a linear stress-strain relationship, giving a total of 8 or 18 Gauss points in the element, as the case may be.

When material non-linearity (plasticity, etc.) affects the element, more integration points are required in the depth of the plate (ξ direction). In such an instance, Simpson's rule has been used for integration through the depth, for which the accuracy is acceptable. It is also convenient in use because of equally spaced intervals (or sampling points). Fig. 3 shows two Gauss stations in the thickness direction, as normally used for linear material behaviour.

Further details of the integration procedure used are given by Kusters [10] and Tolman [13].

b. *Reduced integration and accuracy*

It has been found [11, 12] that since the element used has been degenerated from a finite sized three dimensional isoparametric element, the formulation contains some spurious transverse shear energy terms not present in conventional plate or shell bending theory and produces an over stiff element (or locking). This inaccuracy increases as the shell element becomes thinner. In the case of the chosen element, it has been found [11, 12] that by using the 2×2 Gaussian quadrature rule in the ξxn axes the shear strain is correct at these points for linearly varying moments as well as constant moments in the element, suppressing the spurious transverse shear effects.

All the numerical examples presented in this paper are therefore carried out with 2×2 Gaussian quadrature (4 Gauss points) in the ξxn axes for all integration of the energy terms.

14 Bench mark tests

A number of tests [15] have been carried out to check the analytical tool for the linear and non-linear behaviour. However, in this paper only a few of the more interesting non-linear cases are presented.

14.1 *A cylindrical shell segment*

The fully clamped cylindrical shell segment loaded incrementally by a uniformly distributed gravity load "q" (see Fig. 4 for details) has been used as a standard case for testing geometrical non-linearity by many authors, because no material non-linearity is present. Crisfield [16] presents a range of incremental values of uniformly distributed load versus central deflection ratios from other finite element formulations. Therefore, this range, together with Crisfield's results, are compared with those obtained from computer program DIANA (see Fig. 5). The number of Newton-Raphson iterations required for convergence are shown for each incremental step.

The results in the stable region are close to the lower end of the range, but in the region of the higher non-linearity, the three dimensional effect gives higher values of the plot.

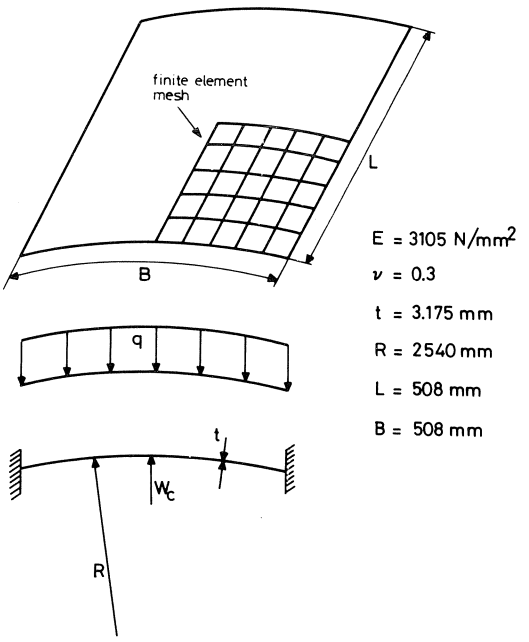

Fig. 4. Fully clamped cylindrical shell under uniformly distributed load.

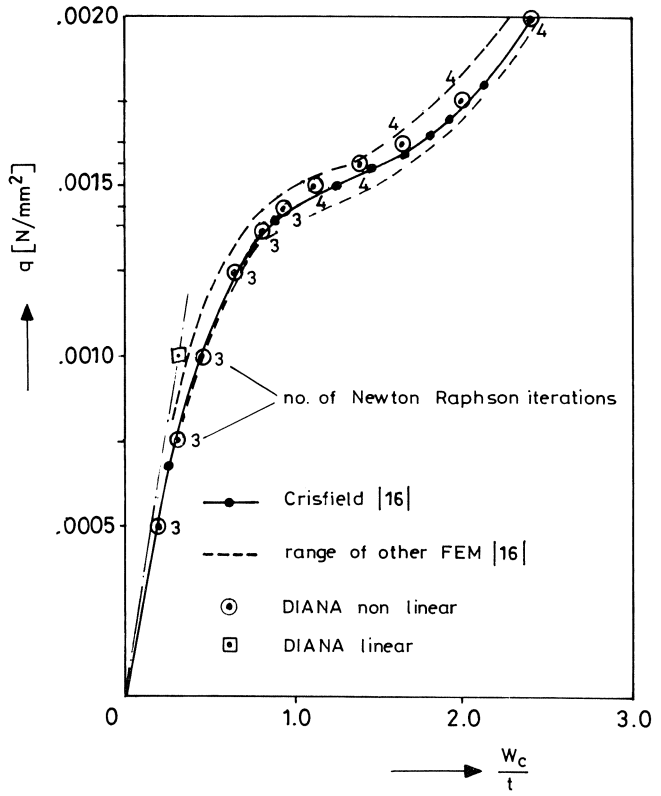

Fig. 5. Results of the linear and geometrical non-linear analysis for the fully campled cylindrical shell.

14.2 *Combined material and geometrical non-linearity of tubular steel T-joints - comparison with experiments*

Akiyama et al. [17] provided data on the load-deflection plots measured up to and beyond collapse of such T-joints loaded in tension and compression. Only the case in compression is described here, since the experimental results for the case in tension had a wide scatter, possibly because of the influence of the weld at the intersection.

Fig. 6 shows the details of the experimental arrangement for the T-joint, where "δ" are positions where deflections were measured. The material properties of the chord and brace are:

Yield stress in the chord in the longitudinal direction $(\sigma_{e_0}) = 392$ N/mm^2
Yield stress in the chord in the transverse direction $(\sigma_{e_0} \times 0.85) = 333$ N/mm^2
Yield stress in the brace in the longitudinal direction $(\sigma_{e_1}) = 441$ N/mm^2
Modulus of elasticity $(E) = 210\,000$ N/mm^2 (assumed)
Poisson's ratio $(\nu) = 0.3$ (assumed)

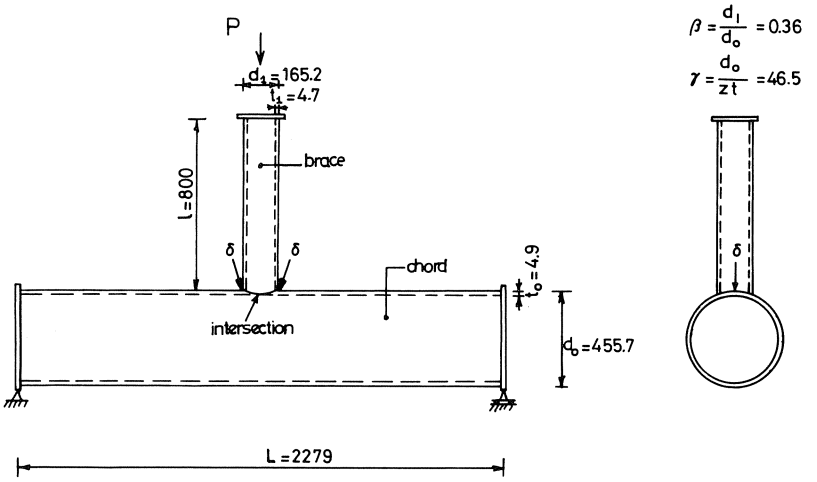

Fig. 6. Details of the T-joint loaded in compression (δ = position where deflection is measured).

Fig. 7 shows the finite element idealization used for the analysis, where the mesh is refined at the intersection because of the stress concentration. The mesh at the intersection in Fig. 7 shows 20 element in the circumference. Assuming symmetry, only a quater of the structure in Fig. 7 has been analysed, allowing 5 elements to be considered along the intersection line. A linear analysis with a coarse mesh idealization of 3 elements along the intersection line, when compared with a linear analysis of the present 5 element

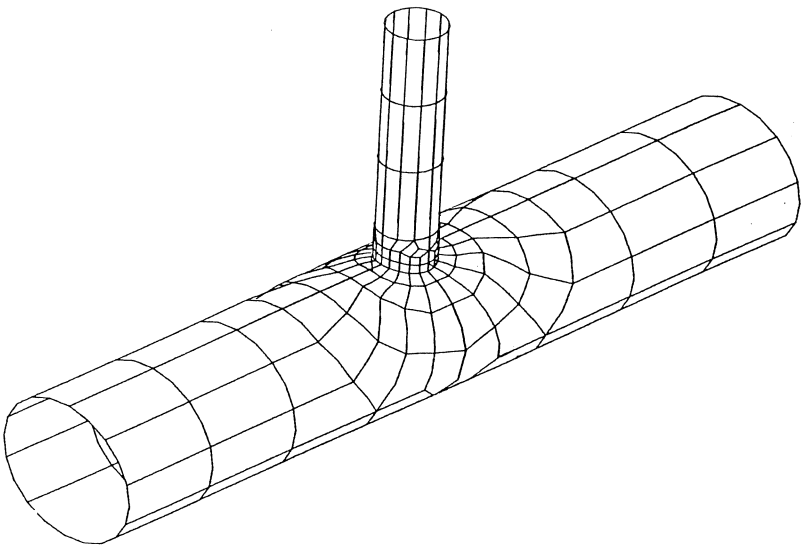

Fig. 7. Computer model of complete T-joint represented by 8 node finite elements.

mesh along the intersection line gave acceptable convergence in the values. However, it was decided to work with the finer mesh so that material and geometric non-linearity could be better represented.

The increments of load were applied by uniformly prescribed displacements at the top of the brace (Figs. 6 and 7). Each end of the chord is assumed to be attached to an infinitely rigid flange plate which is allowed to rotate and move laterally, but not vertically.

Fig. 8 gives the results of the load-displacement plot for the experimental work by Akiyama et al. [17]. The numerical results for the linear-elastic, geometrically non-linear (only) and the combined geometrical and material non-linear cases are also plotted for reference. The combined geometrical and material non-linear results are, however, representative of the real case, and compares well with the experimental values (only 1% higher than the experimental collapse load). The drop off in the computed load displacement plot after maximum load is steeper than the experimental plot. This is because an ideally elastic, perfectly plastic stress-strain relationship was assumed. The only information available was yield stress measured by coupon tests, and the strain hardening properties of the cold worked tubular members were not provided.

The load deflection plots for the isolated geometrical or material non-linear cases were not taken much beyond the experimental collapse load, as they are not relevant.

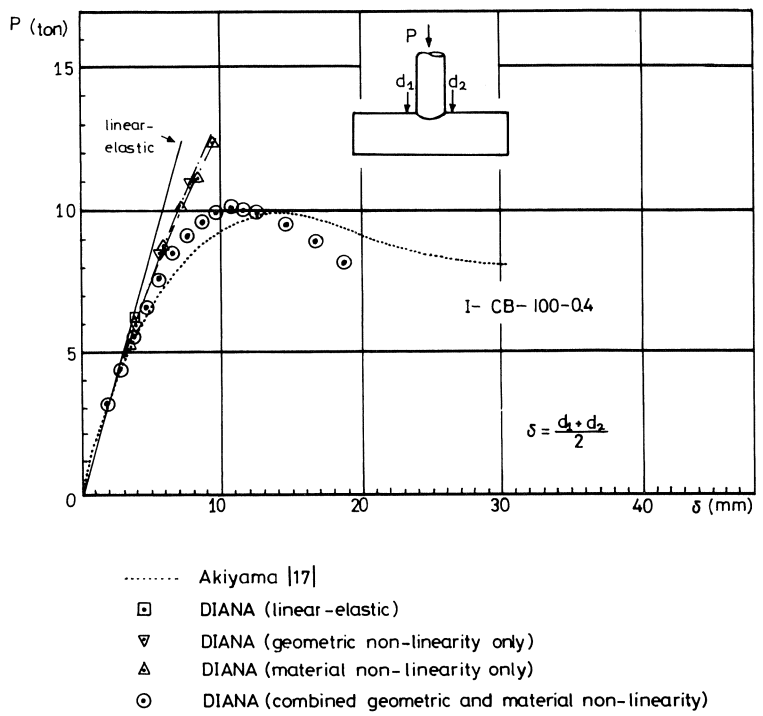

Fig. 8. Load-deflection relationship of the T-joint with brace in compression.

Only 3 integration points using Simpson's rule were taken across the depth of the plate. This is not always considered sufficient to describe the material non-linear behaviour. However, because plasticity was confined to a small area close to the intersection and occurred late in the loading process, it is not thought to have greatly influenced the load-deflection relationship or the collapse behaviour. Fig. 9 shows the spread of plasticity (Von Mises yield criterion) in the chord just after collapse. The semi circular part that was analysed is shown with the elements developed out into a flat rectangular surface for convenience in presentation.

15 Conclusions

The analytical procedure described in the preceding pages is built into the general purpose finite element computer program "DIANA" (DIsplacement ANAlysis) written by IBBC-TNO.

Comparisons of the analytical procedure with other numerical solutions in the linear elastic and non-linear range have shown good correlation, of which only one standard example is presented. Comparison of experimental observations of the load displacement relationship of a tubular T-joint up to and beyond collapse with the analytical behaviour have also given good agreement. The analytical collapse load is 1% higher than the experimental value.

Although the present procedure is capable of handling very large displacements and

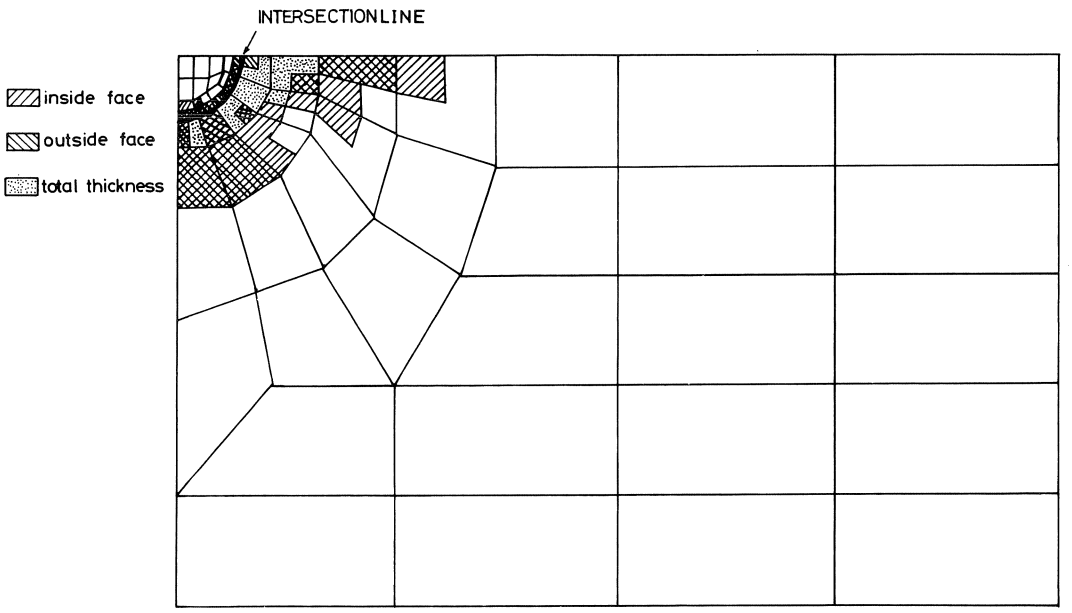

Fig. 9. Von Mises yield on the developed surfaces of the T-joint chord, with brace in compression.

rotations, most Civil Engineering applications, particularly with reference to shell structures, are not concerned with magnitudes where the structure is no longer serviceable. Therefore, although the analytical procedure is capable of handling such cases, examples of this nature have not been investigated here.

16 Acknowledgements

The author wishes to thank his colleagues G. M. A. Kusters and P. Nauta of the department of modern computer techniques for incorporating the non-linear element formulation within computer program DIANA and a useful collaboration. The author also wishes to acknowledge the cooperation of F. S. K. Bijlaard and H. G. A. Stol in applying the formulation to the problems discussed [14]. The numerical comparisons were carried out in connection with the Netherlands Marine Technological Research (Marine Technologisch Speurwerk, MaTS) for the Netherlands Industrial Council for oceanology (industriële Raad voor de Oceanologie, IRO) and sponsored by the Ministry of Economic Affairs (Ministerie van Economische Zaken) and the Steel Industry (Staalbouwkundig Genootschap).

17 References

1. De Witte, F. C. and G. M. A Kusters, Software engineering aspects of flexible structural analysis systems. IABSE Colloquium on Advanced Mechanics of Reinforced Concrete, Delft, June 2-4, 1981.
2. Kirchhoff, G. Über das Gleichgewicht und die Bewegung einer elastischen Scheibe. Journal für reine und angewandte Mathematik, Vol. 40, 1850, p. 51-88.
3. Mindlin, R. D., Influence of rotary inertia and shear on flexural motion of isotopic, elastic plates. Journal of Applied Mechanics, March 18, 1951, no. 1, p. 31-38.
4. Reissner, E., The effect of transverse shear deformation on the bending of elastic plates. Journal of Applied Mechanics, June 1945, A69-A77.
5. Ammad, S., B. M. Irons and O. C. Zienkiewicz, Analysis of thick and thin shell structures by curved finite elements. International Journal for Numerical Methods in Engineering, Vol. 2, 1970, p. 419-451.
6. Ramm, E., A plate/shell element for large deflections and rotations. Formulations and Computational Algorithms in Finite Element Analysis. K. S. Bathe, J. T. Oden and W. Wunderlich (editors), M.I.T. Press 1977.
7. Krakeland, B., Non-linear analysis of shell using degenerate isoparametric elements. Finite Elements in Non-linear Mechanics, Vol. 1. Bergan, et al. (eds.), August 1977, Tapir Press, Trondheim, Norway.
8. Bathe, K. J. and S. Bolourchi, A geometric and material non-linear plate and shell element. Computers and Structures, Vol. 11, p. 23-48, 1980.
9. Zienkiewicz, O. C., The Finite Element Method in Engineering Science, Third Edition, McGraw-Hill, London, 1977.
10. Kusters, G. M. A., Niet-lineair materiaalgedrag van gewapend beton met behulp van de eindige elementenmethode (non-linear material behaviour of reinforced concrete with the help of the finite element method). Report no. BI-77-36/07.1.22110, Institute TNO for Building Materials and Building Structures (in Dutch).
11. Zienkiewicz, O. C., R. L. Taylor and J. M. Too, Reduced integration techniques in general analysis of plates and shells. International Journal for Numerical Methods in Engineering, Vol. 3, 1971, p. 275-290.
12. Pawsey S. F. and R. W. Clough, Improved numerical integration of thick shell finite elements. International Journal for Numerical Methods in Engineering, Vol. 3, 1971, p. 575-586.
13. Tolman, F. P., Some numerically integrated elements for DIANA. Report no. BI-75-0/07.1.102, Institute TNO for Building Materials and Building Structures.
14. Nayak, G. C. and O. D. Zienkiewicz, Elasto-plastic stress analysis. A generalisation for constitutive relations including strain softening. International Journal for Numerical Methods in Engineering, Vol. 5, 1972, p. 113-135.
15. Stol, H. G. A., F. S. K. Bijlaard and R. S. Puthli, Determination of strength and stiffness of welded tubular T-joints up to and beyond collapse with the finite element program DIANA. Report no. B-81-96/63.6.0678, Institute TNO for Building Materials and Building Structures, The Netherlands.
16. Crisfield, M. A., A faster modified Newton-Raphson iteration. Computer Methods in Applied Mechanics and Engineering, 20 (1979) p. 267-268.
17. Akiyama, H. et al. Experimental study on strength of joints in steel tubular structures. J.S.S.C., Vol. 10, No. 102, 1974, 6, p. 37-64 (in Japanese).